Journal of
Applied Remote Sensing

Influence of vertical distribution of phytoplankton on remote sensing signal of Case II waters: southern Caspian Sea case study

Mehdi Gholamalifard
Abbas Esmaili-Sari
Aliakbar Abkar
Babak Naimi
Tiit Kutser

Influence of vertical distribution of phytoplankton on remote sensing signal of Case II waters: southern Caspian Sea case study

Mehdi Gholamalifard,[a] Abbas Esmaili-Sari,[a] Aliakbar Abkar,[b] Babak Naimi,[c] and Tiit Kutser[d]

[a]Tarbiat Modares University, Department of Environment, Faculty of Natural Resources, P.O. Box 46414-356, Noor, Mazandaran, Iran
gholamalifard@gmail.com

[b]K. N. Toosi University of Technology, Faculty of Geodesy and Geomatics Engineering, P.O. Box 15875-4416, Tehran, Iran

[c]Faculty of Geo-Information Science and Earth Observation, P.O. Box 217, 7500 AE, Enschede, The Netherlands

[d]University of Tartu, Estonian Marine Institute, Mäealuse 14, Tallinn 12618, Estonia

Abstract. Reliable monitoring of coastal waters is not possible without using remote sensing data. On the other hand, it is quite difficult to develop remote sensing algorithms that allow one to retrieve water characteristics (like chlorophyll-a concentration) in optically complex coastal and inland waters (called also Case II waters) as the concentrations of optically active substances (phytoplankton, suspended matter, and colored dissolved organic matter) vary independently from each other and the range of variability is often high. Another problem related to developing remote sensing algorithms for retrieving concentrations of optically active substances in such complex waters is vertical distribution of these substances. For example, phytoplankton distribution in the water column is often characterized with maxima just below the surface mixed layer, and some phytoplankton species even have the capability to migrate in the water column and tend to form layers at depths optimal for their growth. Twenty-three field campaigns were performed during the spring-summer period in the coastal waters of the southern Caspian Sea where vertical distribution of phytoplankton was measured by means of chlorophyll-a fluorometer. There results showed that there is usually a chlorophyll-a maximum between 10 and 20 m where the concentration is about one order of magnitude higher than in the top mixed layer. The Hydrolight 5.0 radiative transfer model used to estimate if the vertical distribution of biomass have detectable impact on remote sensing signal in these waters. For that purpose, several stations with distinctly different chlorophyll-a profiles were selected and two simulations for each of those measuring stations was carried out. First the Hydrolight was run with the actual chlorophyll-a vertical distribution profile and second a constant chlorophyll-a value (taken as an average of measured chlorophyll-a in the surface layer) was used in the model simulation. The modelling results show that the "deep" chlorophyll maximum has negligible effect on the remote sensing reflectance spectra. Consequently, there is no need to take into account the vertical distribution of phytoplankton while developing remote sensing algorithms for the Caspian Sea coastal waters. [DOI: 10.1117/1.JRS.7.073550]

Keywords: chlorophyll-a; vertical distribution; hydrolight; Case II waters; southern Caspian Sea.

Paper 13041 received Feb. 14, 2013; revised manuscript received Apr. 11, 2013; accepted for publication Apr. 19, 2013; published online Jun. 3, 2013.

1 Introduction

Coastal waters occupy at the most 8–10% of the ocean surface and only 0.5% of its volume, but represent an important fraction in terms of economic, social, and ecological value.[1] Coastal waters are also under the greatest anthropogenic pressure. As a result, there is strong need

to monitor coastal environments. By monitoring changes in water quality we can observe, assess, and correct long term trends in water quality degradation. It is obvious that the infrequent measurements from research vessels or automated measuring systems on ships of opportunity or buoys cannot provide the spatial and temporal coverage needed for monitoring such dynamic environments like coastal waters.[2] Remote sensing can provide greater spatial coverage with finer spatial resolution and often with good temporal frequency. This makes remote sensing a rich source of data.[3]

The remote sensing signal is determined by the amount of optically active substances like phytoplankton (usually measured as concentration of chlorophyll-a), suspended matter, and colored dissolved organic matter (CDOM). In optically simple oceanic waters, the latter two are well correlated with the phytoplankton as they are phytoplankton degradation products. In optically complex coastal and inland waters, commonly labelled as "Case II" waters,[4] most of the CDOM and suspended matter originates from the adjacent land. As a result, the concentrations of these substances vary independently from each other and they may vary across a wide range (orders of magnitude). Therefore, the developing of reliable remote sensing algorithms for such waters is very complicated and the algorithms are often local or even seasonal.

Another complicating aspect is vertical distribution of the optically active substances. For example, CDOM transported into marine environment by rivers may stay on the sea surface as the fresh water is lighter than the salt water.[5] These effects are limited to very near coastal zone. On the other hand vertical distribution of phytoplankton may have quite significant impact on remote sensing signal over large areas. Others have shown that the vertical distribution of phytoplankton and the deep chlorophyll maximum in oceanic waters has an impact on the remotely sensed signal.[6,7] In turbid coastal waters, the depth of penetration of light (the depth where remote sensing signal is formed) is often relatively shallow (a few meters to centimeters). On the other hand Kutser et al.[8] have shown that vertical distribution of phytoplankton may have significant impact on the remote sensing signal. Especially in the case of cyanobacteria that can regulate their buoyancy and migrate in water column to the depth optimal for their growth.

There is little information available about the vertical distribution of chlorophyll-a in the southern Caspian Sea. In the southern Caspian Sea the thermocline starts to form in spring, sharpens in summer, begins to degrade and then completely degrades in autumn. It is usually not observed at all in winter.[9] The formation and destruction of seasonal thermocline affects the chlorophyll-a concentration. The aim of our study was to measure the vertical distribution of phytoplankton (chlorophyll-a) in the southern Caspian Sea during the period when the thermocline is formed and to evaluate whether the vertical distribution of phytoplankton has an impact on the remote sensing signal complicating development of the chlorophyll-a retrieval algorithms for the coastal waters of the Caspian Sea.

2 Methods

2.1 *Field Measurements*

Field sampling was conducted in the southern Caspian Sea waters crossing a full freshwater-marine water gradient (Fig. 1). Twenty-three cruises were conducted in thirty stations during spring-summer period of 2011. The vertical profile of chlorophyll-a was measured using a seapoint chlorophyll fluorometer (SCF) that was interfaced with an Idronaut OCEAN SEVEN 316 CTD multiparameter probe. SCF is a high-performance, low power instrument for *in situ* measurements of chlorophyll-a. Also, the vertical profile of water turbidity was measured using an optical probe (Seapoint Turbidity Meter). This instrument measures light scattered by particles suspended in water generating an output voltage proportional to turbidity or the amount of suspended solids. The results are expressed in Formazine Turbidity Units (FTU), which may be directly related to the suspended sediment concentration.[10]

The amount of total suspended solids, TSS, was measured by filtering 1 L water samples through preweighed 47 mm Millipore GN filters (0.45 μm pore size). Filters were dried in a desiccator and weighed again. The difference of filter weights before and after filtering the

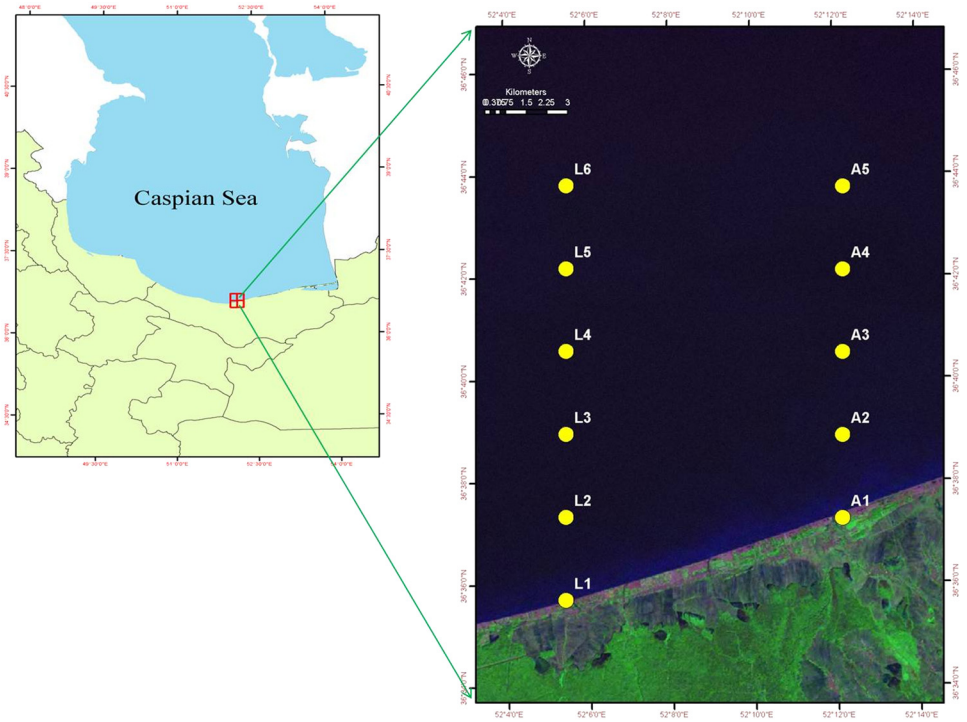

Fig. 1 Sampling stations in the southern Caspian Sea. (There are five stations in two transects, the stations are named according to L1, L2, L3, L4, L5, A1, A2, A3, A4, A5. The distance between stations is 3 km and between two transects is 10 km).

water sample, together with the volume of filtered seawater, was used to calculate the TSS concentration.[11]

For CDOM, seawater was filtered the same day after returning to laboratory (Central Laboratory, Faculty of Natural Resources, Tarbiat Modares University) through polycarbonate track etch membrane filters (PCMembran, 0.2 μm, 47 mm) (Sartorius-stedium). CDOM absorbance was determined between 200 nm and 850 nm using a Perkin Elmer Lambda 25 spectrophotometer in a 10 cm quartz cuvette. The Milli-Q water was used as reference and a baseline correction was applied to the data by subtracting the average between 683 nm and 687 nm to the entire spectrum.[12,13] The absorbance values at each wavelength were transformed into absorption coefficients using

$$a_{\mathrm{CDOM}}(\lambda) = 2.303 * \frac{\mathrm{OD}_{\mathrm{CDOM}}(\lambda)}{l},$$

where l is the cuvette path length (0.1 m).

Absorption data were fitted with an exponential function using nonlinear regression between 350 nm and 500 nm[12–14] to retrieve $a_{\mathrm{CDOM}}(\lambda_r)$, the CDOM absorption estimate at a reference wavelength (375 nm) and S, the slope of the absorption curve:

$$a_{\mathrm{CDOM}}(\lambda) = a_{\mathrm{CDOM}}(\lambda r) * \exp[-S(\lambda - \lambda r)].$$

The absorption value at 375 nm, $a_{\mathrm{CDOM}}(375)$, was chosen to quantify CDOM.[13–15]

2.2 *Optical Modelling*

The HydroLight 5.0 radiative transfer code[16] was used to simulate the remote sensing reflectance spectra. The HydroLight radiative transfer numerical model computes radiance distributions and related quantities. Users can specify the water absorption and scattering properties, the sky conditions, and the bottom boundary conditions. HydroLight then solves the scalar radiative transfer

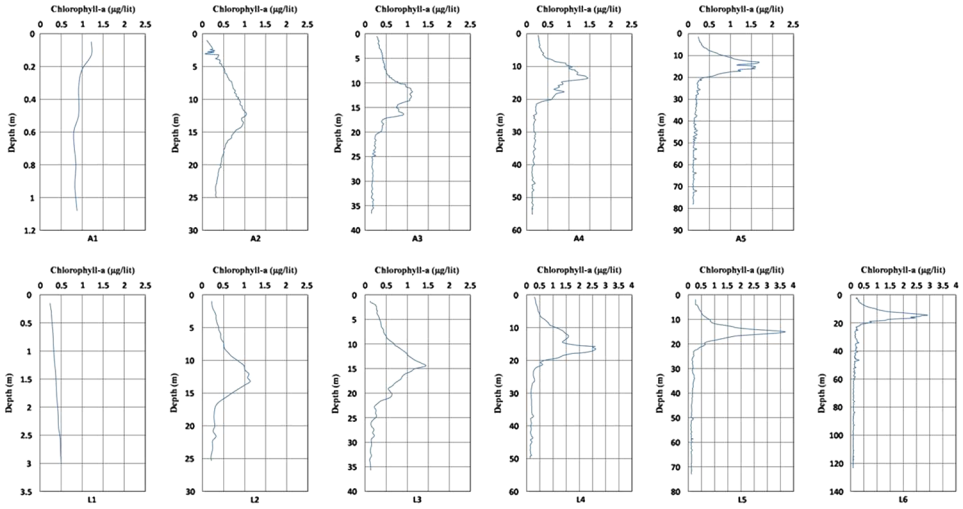

Fig. 2 Vertical profile of chlorophyll-a measured in different stations (Cruise Date: 2011-07-31).

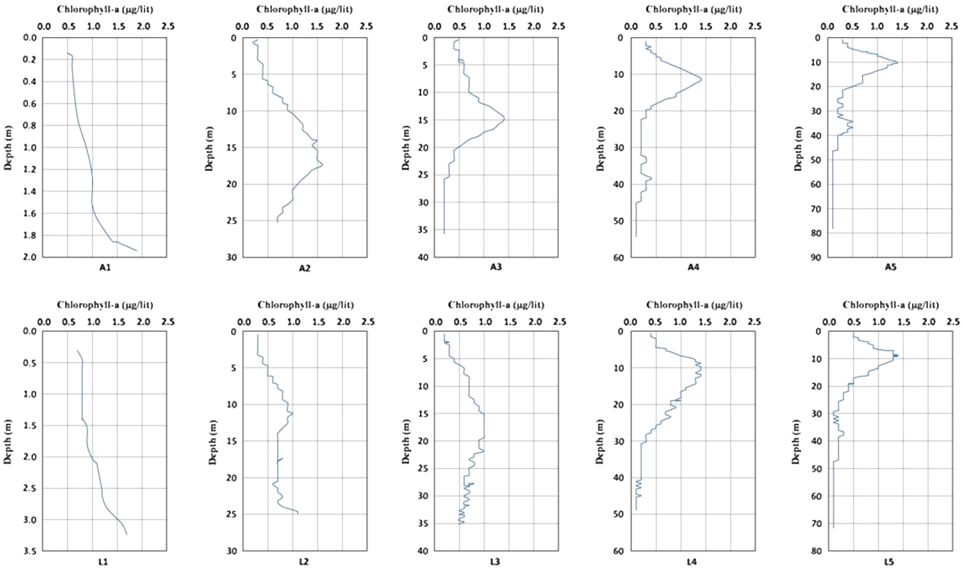

Fig. 3 Vertical profile of chlorophyll-a measured in different stations (Cruise Date: 2011-08-17).

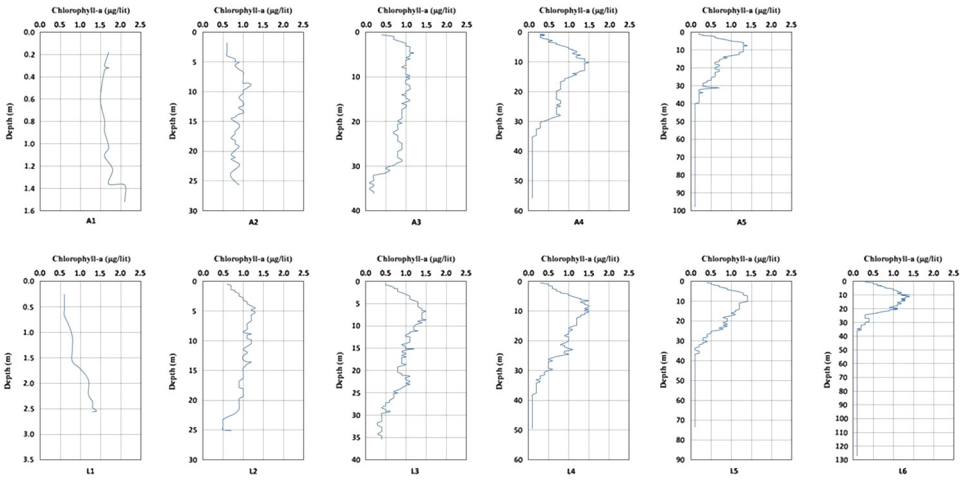

Fig. 4 Vertical profile of chlorophyll-a measured in different stations (Cruise Date: 2011-09-15).

Table 1 The results of field measurements of optically active constituents.

Date	Stations	Depth (m)	Chlorophyll (μg/l)	TSS (mg/L)	a CDOM (375) (1/m)	S
31 July 2011						
	A1	1.30	1.6	29.40	1.602888	0.0127
	A2	25.50	0.3	2.06	0.458297	0.0155
	A3	37.80	0.56	2.15	0.607992	0.0167
	A4	58.20	0.56	2.19	0.278663	0.0176
	A5	98.09	0.42	0.48	0.485933	0.0178
	L1	77.00	1.22	14.78	2.547118	0.0135
	L2	51.40	0.58	3.77	1.56604	0.0129
	L3	36.90	0.92	1.56	1.33574	0.0123
	L4	51.40	0.6	2.21	1.19756	0.0112
	L5	77.00	0.62	1.37	1.039848	0.0118
17 August 2011						
	A1	2.20	1.4	71.27	0.511266	0.0168
	A2	26.30	0.6	0.64	0.269451	0.0174
	A3	37.20	1	0.55	0.267148	0.0173
	A4	57.30	0.6	0.64	0.34545	0.0162
	A5	98.15	0.6	0.64	0.375389	0.0174
	L1	3.40	1.6	35.73	3.518984	0.0109
	L2	25.60	0.6	2.01	1.01332	0.0124
	L3	35.70	0.4	0.74	0.978775	0.0131
	L4	51.40	0.8	0.97	1.001805	0.0129
	L5	75.70	1	1.10	1.319619	0.0136
15 September 2011						
	A1	1.52	3	85.43	1.213681	0.0159
	A2	25.90	1.2	12.34	1.011017	0.0156
	A3	37.20	0.8	3.89	0.50666	0.0175
	A4	57.60	0.6	1.84	0.446782	0.0173
	A5	97.70	0.4	1.67	0.467509	0.0173
	L1	2.60	1.2	31.44	0.379995	0.0173
	L2	25.60	1.2	4.92	0.393813	0.0174
	L3	38.30	1	7.02	0.375389	0.0174
	L4	51.20	0.6	6.70	0.377692	0.0175
	L5	75.60	0.8	7.02	0.416843	0.0173

equation (RTE) to compute the in-water radiance as a function of depth, direction, and wavelength. Other quantities of interest, such as the water-leaving radiance and remote-sensing reflectance, are also obtained from the computed radiances. Caspian Sea waters belong to optically more complex Case II waters where the concentrations of optically active substances vary independently of chlorophyll-a.

A Case II water model with three optically active substances (chlorophyll-a, CDOM and mineral particles) was parameterized for the Caspian Sea study in HydroLight. The mass-specific absorption and scattering coefficients of optically active substances available in the HydroLight were used as there is no information about those parameters in the Caspian Sea. The modelling was carried out over the wavelength range of 350-850 nm with 5 nm intervals. Wind speed was taken to be 2 $m \cdot s^{-1}$. The solar zenith angle was assumed to be 30 deg, which is typical for the time around midday in the July-August period when the thermocline occurs in the Caspian Sea.

Eleven measuring stations were selected for the modelling study in order to describe the whole range of variability in vertical distribution of biomass as it was observed during our field campaigns. Two different HydroLight runs were made for each of the selected stations. First we used a measured chlorophyll profile (Figs. 2, 3, and 4) for each station. A second model run for each station was carried out using a constant chlorophyll-a value for the whole water column. An average chlorophyll-a of the top first meter was used for the whole water column.

3 Results and Discussion

Table 1 shows the results of field measurements of optically active constituents in three cruises. As expected, $a_{CDOM}(375)$ of nearer stations to the coast show much higher values compared to far stations in each cruise, i.e., $0.37 - 3.51\ m^{-1}$ and $0.37 - 1.31\ m^{-1}$ respectively. TSS concentration ranged from $14.87 - 85.43\ mg/l$ in near stations to coast to $0.48 - 7.02\ mg/l$ in the far stations from the coast. Chlorophyll showed variations, too. Near stations to the coast show much higher values compared to far stations in each cruise, i.e., $1.2 - 3\ mg/m^3$ and $0.4–1\ mg/m^3$ respectively (Table 1).

Figures 5 to 10 provide some more detailed insight into formation of the reflectance spectra revealed by the model simulations. Figures 5 and 6 show the total absorption coefficient and its components and total absorption coefficients just beneath the sea surface for two stations (A1 near to the coast, A5 far from the coast), and Figures 7 and 8 show the corresponding scattering coefficient and its components for July 2011. The total absorption is dominated by mineral

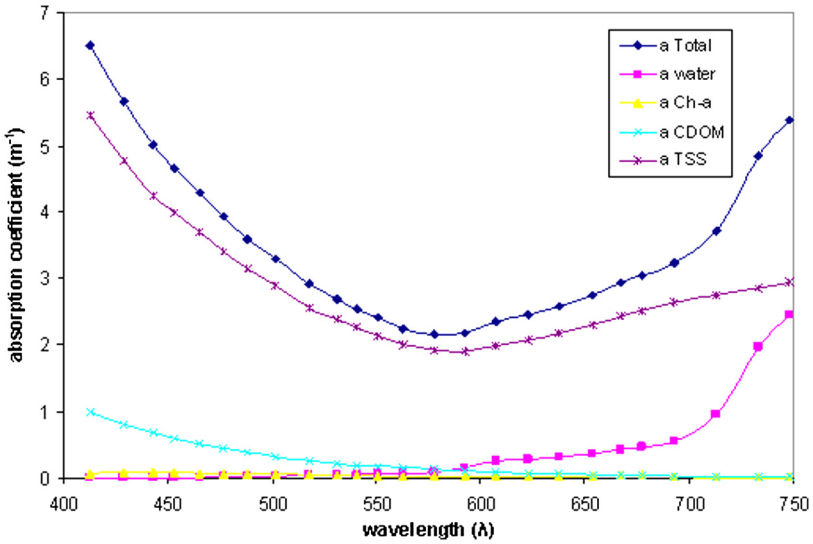

Fig. 5 Absorption coefficients for the station A1 (near to the coast).

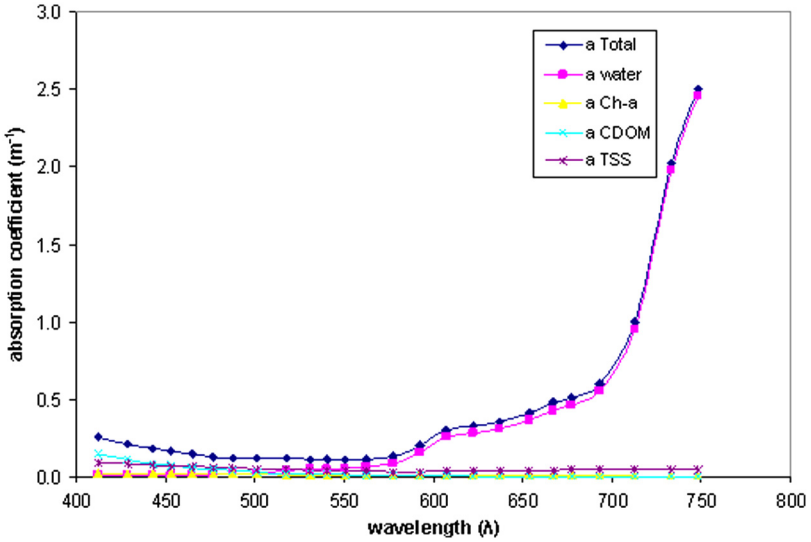

Fig. 6 Absorption coefficients for the station A5 (far from the coast).

particles in near stations to the coast and by the water itself in stations far from the coast. The primary scatters are mineral particles in near stations to the coast and chlorophyll-a in stations far from the coast, too. However, the water makes only a small contribution to the total scattering.

The irradiance reflectance and remote-sensing reflectance R_{rs}, the quantity of interest for "ocean color" remote sensing, is shown in Figs. 9 and 10. As can be seen, R values become higher as turbidity increases.

In this study, we assumed that the impact of vertical distribution of phytoplankton is detectable by remote sensing instruments if the difference between the two modelled spectra is higher than the signal to noise ratio of different sensors. This kind of methodology has been used to estimate if potentially toxic cyanobacterial blooms be separated from blooms of other algae,[17] if remote sensing can be used to map benthic habitats in coastal waters[18] and determining what type of coral reef habitats can be separated from each other.[19]

Figures 11 and 12 illustrate the influence of the vertical distribution of chlorophyll-a on the remote sensing signal in two stations (A3 & A5). Using the constant chlorophyll-a value through the water column produces slightly higher reflectance values than using actually measured chlorophyll-a profiles. This indicates that the vertical distribution of phytoplankton biomass has a small impact on the reflectance spectra. However, the difference between the reflectance

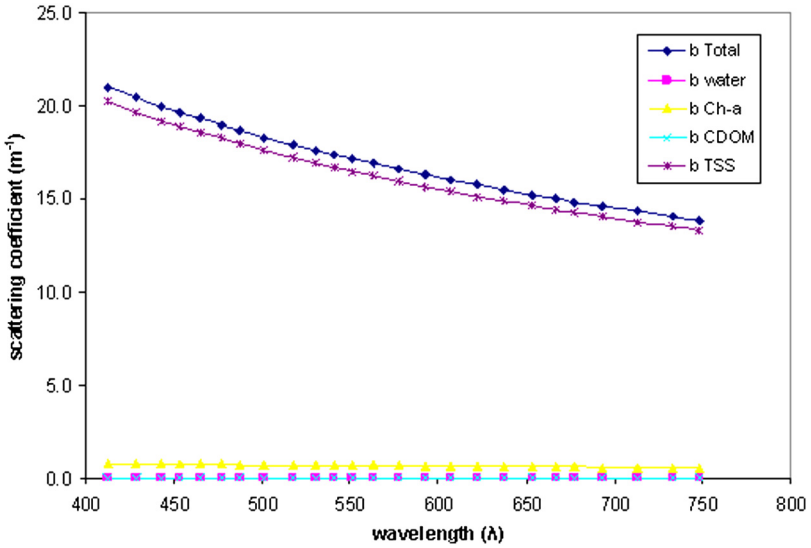

Fig. 7 Scattering coefficients for the station A1 (near to the coast).

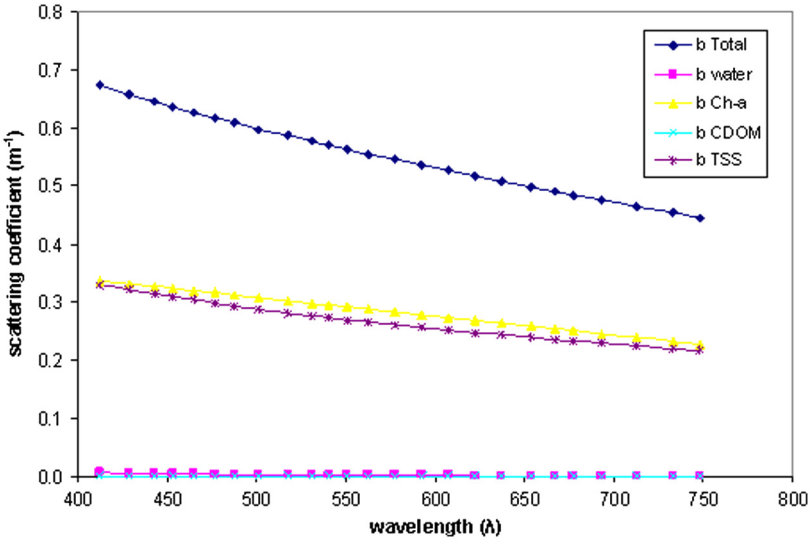

Fig. 8 Scattering coefficients for the station A5 (far from the coast).

calculated for a homogeneous water column and the reflectance calculated for the actual stratification of biomass is so small that no remote sensing sensor can detect the difference.

This result is not surprising if one considers that the contribution of different water layers to the total remote sensing signal decreases exponentially with increasing depth. Our estimates show that the depth of penetration (the layer from which the remote sensing signal originates) is less than 18 m (based on $2.3/K_d$) in the clearest station of study area (Fig. 13). The deep chlorophyll maximum is in deeper waters than the depth of penetration in all stations. It means that the order of magnitude increases in phytoplankton concentration cannot have impact on the remote sensing signal since the biomass peak is below the layer remote sensing sensors can "see."

The field measurements were carried out during the spring-summer period (May–September) when thermocline should occur in the southern Caspian Sea waters. During the rest of the year, the top layer of the sea is well mixed and the vertical distribution of biomass is homogenous.

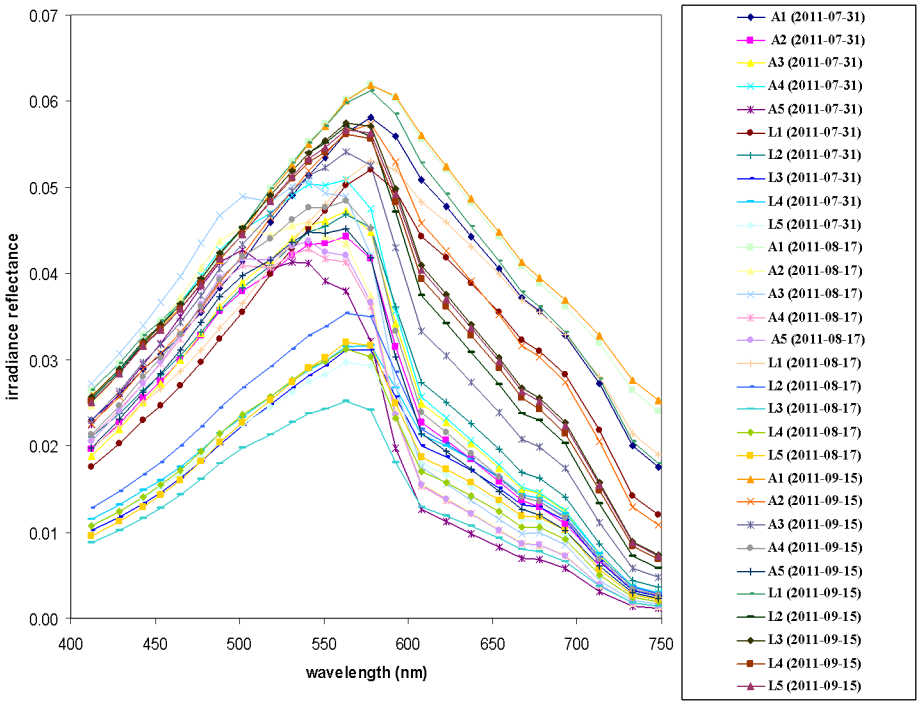

Fig. 9 Irradiance reflectance for the water body.

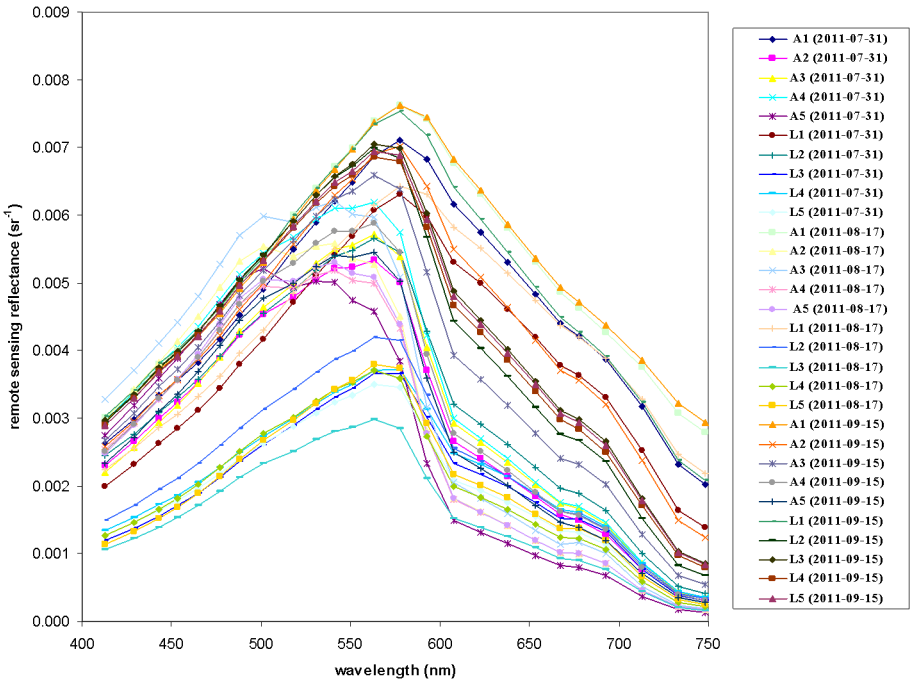

Fig. 10 Remote sensing reflectance for the water body.

Therefore, our measurements should describe the range of variability in vertical distribution of phytoplankton occurring in the southern Caspian Sea.

The results show that the impact of vertical distribution of phytoplankton biomass is very small in the cases where the nonuniform distributions occur. Remote sensing sensors cannot detect such a small difference. It means that taking a surface water sample for calibration and validation of remote sensing algorithms is sufficient in the southern Caspian Sea to characterize the water mass under investigation. We are planning to validate different chlorophyll-a (and other water characteristics) retrieval algorithms for the southern Caspian Sea and develop better regional algorithms if needed. The negligible impact of the deep chlorophyll maximum on the remote sensing signal suggests that only the concentrations and specific optical properties of the optically active substances (and not their vertical distribution) have to be taken into account when developing regional algorithms for retrieval of water characteristics in the southern Caspian Sea.

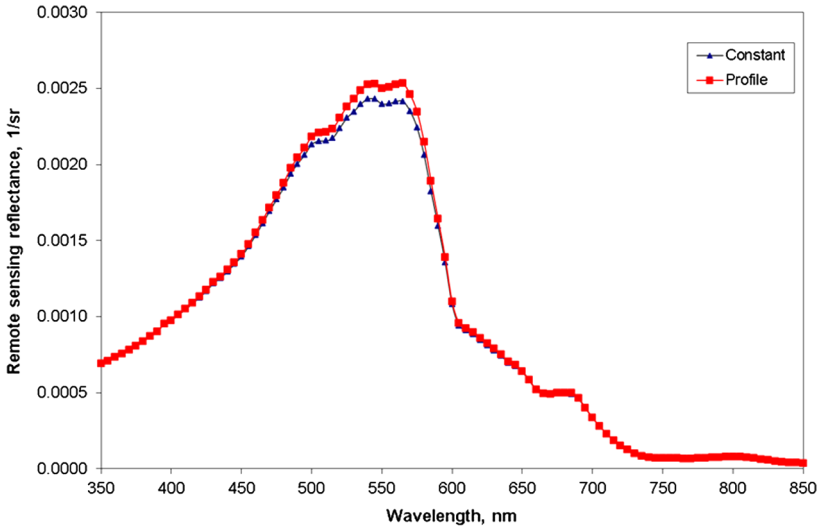

Fig. 11 Modelled remote sensing reflectance in Station A3 using the constant chlorophyll-a value through the water column and actually measured chlorophyll-a profiles.

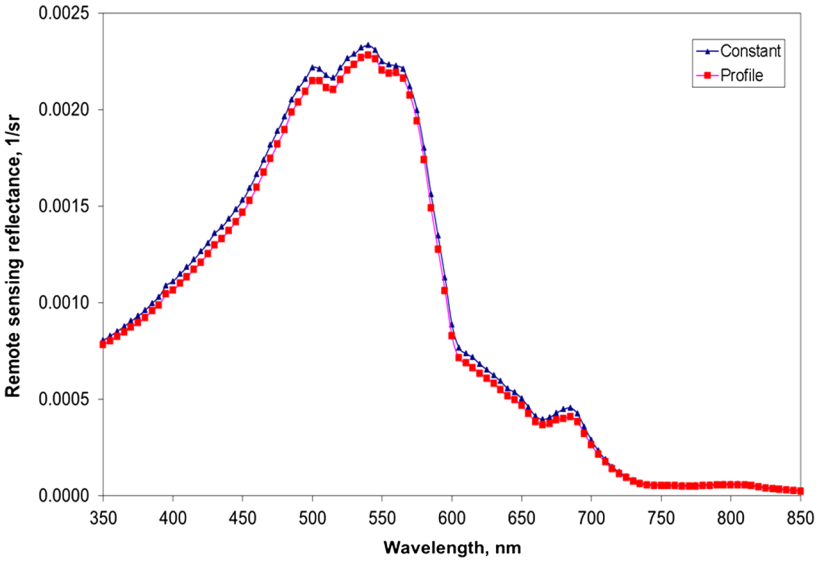

Fig. 12 Modelled remote sensing reflectance in Station A5 using the constant chlorophyll-a value through the water column and actually measured chlorophyll-a profiles.

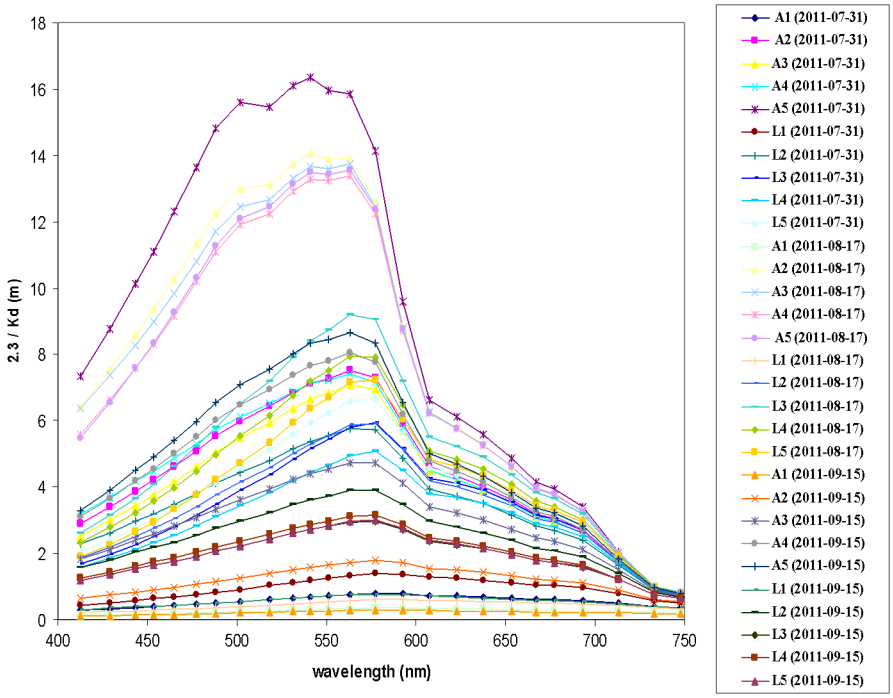

Fig. 13 Upper two diffuse attenuation depths [a depth of 2.3/Kd (λ)] in different cruises.

Acknowledgments

The study presented here is part of the dissertation in partial fulfillment of the requirements for the degree of PhD in Tarbiat Modarres University (TMU) of Iran. The authors extend their appreciation for the support provided by the authorities of the Tarbiat Modares University in funding the study and presenting its results in JARS. First and foremost, I would like to express my sincere thanks to Mrs. Mina Emadi Shaibani for supporting and encouraging the research. I am grateful to Dr. Nemat Mahmoudi for continuing encouragement and support in the preparation of the field data. Also, thanks to Mr. Engr. Mahmoud Valizadeh and

Mr. Gholizadeh for several suggestions concerning sampling affairs. We also thank the anonymous reviewers for their constructive suggestions and comments.

References

1. N. Hoepffner and G. Zibordi, "Remote sensing of coastal waters," *Encyclopedia of Ocean Sciences*, 2nd ed., J. H. Steele, K. K. Turekian, and S. A. Thorpe, pp. 732–741, Elsevier, Amsterdam, The Netherlands (2009).
2. T. Kutser, "Quantitative detection of chlorophyll in cyanobacterial blooms by satellite remote sensing," *Limnol. Oceanogr.* **49**(6), 2179–2189 (2004), http://dx.doi.org/10.4319/lo.2004.49.6.2179.
3. P. Bierman et al., "A review of methods for analysing spatial and temporal patterns in coastal water quality," *Ecol. Indicat.* **11**(1), 103–114 (2011), http://dx.doi.org/10.1016/j.ecolind.2009.11.001.
4. A. Morel and L. Prieur, "Analysis of variations in ocean color," *Limnogy Oceanogr.* **22**(4), 709–722 (1977), http://dx.doi.org/10.4319/lo.1977.22.4.0709.
5. L. A. Clementson et al., "Properties of light absorption in a highly coloured estuarine system in south-east Australia which is prone to blooms of the toxic dinoflagellate Gymnodinium catenatum," *Estuar. Coast. Shelf Sci.* **60**(1), 101–112 (2004), http://dx.doi.org/10.1016/j.ecss.2003.11.022.
6. H. R. Gordon and D. K. Clark, "Remote sensing optical properties of a stratified ocean: an improved interpretation," *Appl. Opt.* **19**(20), 598–600 (1980), http://dx.doi.org/10.1364/AO.19.000598.
7. M. Stramska and D. Stramski, "Effects of non-uniform vertical profile of chlorophyll concentration on remote-sensing reflectance of the ocean," *Appl. Opt.* **44**, 1735–1747 (2005), http://dx.doi.org/10.1364/AO.44.001735.
8. T. L. Kutser, L. Metsamaa, and A. G. Dekker, "Influence of the vertical distribution of cyanobacteria in the water column on the remote sensing signal," *Estuar. Coast. Shelf Sci.* **78**(4), 649–654 (2008), http://dx.doi.org/10.1016/j.ecss.2008.02.024.
9. A. Roohi et al., "Changes in biodiversity of phytoplankton, zooplankton, fishes and macrobenthos in the Southern Caspian Sea after the invasion of the ctenophore Mnemiopsis Leidyi," *Biol. Invas.* **12**(7), 2343–2361 (2010), http://dx.doi.org/10.1007/s10530-009-9648-4.
10. V. Volpe, S. Silvestri, and M. Marani, "Remote sensing retrieval of suspended sediment concentration in shallow waters," *Rem. Sens. Environ.* **115**(1), 44–54 (2011), http://dx.doi.org/10.1016/j.rse.2010.07.013.
11. J. L. Mueller et al., "Ocean optics protocols for satellite ocean color sensor validation: biogeochemical and bio-optical measurements and data analysis protocols," Revision 5, Volume V, NASA/TM-2003, Goddard Space Flight Space Center (2003).
12. M. Babin et al., "Variations in the light absorption coefficients of phytoplankton, nonalgal particles, and dissolved organic matter in coastal waters around Europe," *J. Geophys. Res.* **108**(C7), 3211 (2003), http://dx.doi.org/10.1029/2001JC000882.
13. R. Astoreca, V. Rousseau, and C. Lancelot, "Coloured dissolved organic matter (CDOM) in Southern North Sea waters: Optical characterization and possible origin," *Estuar. Coast. Shelf Sci.* **85**(4), 633–640 (2009), http://dx.doi.org/10.1016/j.ecss.2009.10.010.
14. A. Bricaud, A. Morel, and L. Prieur, "Absorption by dissolved organic matter of the sea (yellow substance) in the UV and visible domains," *Limnol. Oceanogr.* **26**(1), 43–53 (1981), http://dx.doi.org/10.4319/lo.1981.26.1.0043.
15. C. A. Stedmon and S. Markager, "The optics of chromophoric dissolved organic matter (CDOM) in the Greenland Sea: an algorithm for differentiation between marine and terrestrially derived organic matter," *Limnol. Oceanogr.* **46**(8), 2087–2093 (2001), http://dx.doi.org/10.4319/lo.2001.46.8.2087.
16. C. D. Mobley and L. K. Sundman, *Hydrolight 5 Users' Guide*, Sequoia Scientific, Inc., Redmond, WA (2008).
17. L. Metsamaa, T. Kutser, and N. Strömbeck, "Recognising cyanobacterial blooms based on their optical signature: a modelling study," *Boreal Environ. Res.* **11**(), 493–506 (2006).

18. E. Vahtmäe et al., "Feasibility of hyperspectral remote sensing for mapping benthic macroalgal cover in turbid coastal waters," *Rem. Sens. Environ.* **101**(3), 342–351 (2006), http://dx.doi.org/10.1016/j.rse.2006.01.009.
19. T. Kutser, A. G. Dekker, and W. Skirving, "Modelling spectral discrimination of Great Barrier Reef benthic communities by remote sensing instruments," *Limnol. Oceanogr.* **48**(1, part2), 497–510 (2003), http://dx.doi.org/10.4319/lo.2003.48.1_part_2.0497.

Mehdi Gholamalifard is currently a PhD student of environmental pollutions (satellite monitoring) at the Tarbiat Modares University (TMU) in Iran. He received his MSc in environment from TMU, Iran, in 2006 based on his applied research on spatial-temporal modeling of MSW landfill supply and demand using SLEUTH urban growth model (UGM) in a GIS environment. He finished his BSc on environment at IAU-Arak in 22th July 2004. He received full scholarship from the Ministry of Science, Research and Technology to obtain a PhD degree at TMU. Also, he received the Erasmus Mundus research fellowship at the Faculty of Geo-Information Science and Earth Observation (ITC), The Netherlands, in Autumn 2012. His research interest focuses on environmental assessment and modeling, satellite monitoring, and geoinformatics applications in decision making.

Biographies and photographs of other authors are not available.